

# Efficient determination of synchronization domains from observations of asynchronous dynamics

Michael Rosenblum<sup>1,2</sup> and Arkady Pikovsky<sup>1,2</sup>

<sup>1</sup>*Institute of Physics and Astronomy, University of Potsdam, Karl-Liebknecht-Str. 24/25, 14476 Potsdam-Golm, Germany*

<sup>2</sup>*The Research Institute of Supercomputing, Lobachevsky National Research State University of Nizhny Novgorod, 606950, Nizhny Novgorod, Russia*

(Received 20 April 2018; accepted 28 June 2018; published online 3 October 2018)

We develop an approach for a fast experimental inference of synchronization properties of an oscillator. While the standard technique for determination of synchronization domains implies that the oscillator under study is forced with many different frequencies and amplitudes, our approach requires only several observations of a driven system. Reconstructing the phase dynamics from data, we successfully determine synchronization domains of noisy and chaotic oscillators. Our technique is especially important for experiments with living systems where an external action can be harmful and shall be minimized. *Published by AIP Publishing.* <https://doi.org/10.1063/1.5037012>

**It is widely accepted that synchronization plays an important role in various branches of science and engineering and is frequently encountered in living systems. The phenomenon is intensively studied both theoretically and experimentally, and the experiments frequently involve determination of synchronization regions, also known as Arnold tongues. The straightforward determination of the tongues requires slow variation of the frequency and amplitude of the external action and finding the domains where the investigated self-sustained oscillatory system is locked to the acting force. Simple and reliable, this technique, however, requires many measurements and can be quite time-consuming. This limitation may become crucial in experiments with living systems that cannot maintain stationarity for long time intervals, and where extensive external forcing may be destructive. In this paper, we develop a technique for a fast determination of synchronization regions. In fact, a rough estimation can be obtained already from a single observation of the driven system provided it remains asynchronous. This estimation can be essentially improved by a few further measurements.**

## I. INTRODUCTION

A standard problem in the analysis of self-sustained oscillatory systems is the determination of their synchronization properties, in particular inference of synchronization regions, also denoted as Arnold tongues. In the case of an oscillator driven by a force with an amplitude  $\varepsilon$  and a driving frequency  $\nu$ , these regions are domains in the  $\varepsilon, \nu$  plane, where the observed frequency  $\Omega$  of the oscillator becomes equal to  $\nu$  (or, more generally, these frequencies obey the relation  $n\Omega = m\nu$ , where  $n$  and  $m$  are some integers). Practically, these domains can be obtained by scanning  $\nu$  and  $\varepsilon$  over a sufficiently fine grid, and by computing  $\Omega$  for each  $(\nu, \varepsilon)$  pair.

This standard approach goes back to classical experiments by van der Pol and van der Mark<sup>1</sup> and by Appleton,<sup>2</sup>

and it has been exploited within the last three decades in many experiments with periodic, noisy, and chaotic oscillators of different origins, ranging from electronic circuits and lasers to circadian and cardiovascular systems (see Ref. 3 and references therein). Recent examples include experiments with nanomechanical oscillators,<sup>4</sup> organ pipes,<sup>5,6</sup> coupled Boolean phase oscillators,<sup>7</sup> microfluidic drop emitter,<sup>8</sup> synthetic genetic oscillators,<sup>9</sup> cardiovascular system under paced respiration,<sup>10,11</sup> hair cell bundles,<sup>12</sup> brain alpha rhythm in humans,<sup>13</sup> brain gamma-band rhythm in monkeys,<sup>14</sup> thermoacoustic oscillator,<sup>15</sup> spike and wave discharges in rats,<sup>16</sup> and circadian clock.<sup>17</sup>

Thus, the traditional approach requires time-consuming experiments, where a large number of measurements for different values of  $\nu$  and  $\varepsilon$  shall be performed. In this paper, we suggest a technique which essentially simplifies the task of determining the synchronization region, as it requires less measurements. This is especially important if the system to be examined cannot be for a long time isolated from its environment and kept in steady conditions. First, we demonstrate that the synchronization region can be efficiently recovered if only several measurements for each value of the amplitude  $\varepsilon$  are performed. Moreover, for a weak forcing, the Arnold tongue can be computed *from a single measurement*, provided the forced oscillator remains in a quasiperiodic, non-synchronous state. Furthermore, if the oscillator is subject to internal fluctuations—a common situation for all real-world studies—we can recover the synchronization domain of a noise-free system. Finally, we address the case when, in addition to random perturbations, the oscillator is subject to an unobserved force. We also illustrate the approach by an application to a chaotic system.

## II. THE TECHNIQUE

Our starting point is the phase dynamics theory (see, e.g., Refs. 3 and 18), briefly outlined below. Consider an autonomous noisy periodic or a weakly chaotic oscillator.

As is well-known, the dynamics of such a system can be parameterized by the phase  $\varphi(t)$ , which evolves according to

$$\dot{\varphi} = \omega + \zeta(t), \quad (1)$$

where  $\omega$  is the natural frequency of the system and the random term  $\zeta(t)$  accounts for intrinsic fluctuations of the system parameters and/or for the effect of chaos. Consider now the simplest case of external driving when the system is subject to a periodic force  $\varepsilon I(\nu t) = \varepsilon I(\nu t + 2\pi)$ . Then, according to the perturbation theory,<sup>18</sup> for sufficiently small  $\varepsilon$  one can consider variations of the oscillator's amplitude as enslaved, and reduce the description to the phase dynamics.

A general equation for the phase reads

$$\dot{\varphi} = \omega + Q(\varphi, \nu t; \varepsilon, \nu) + \zeta(t). \quad (2)$$

Here,  $Q$  is the coupling function; it quantifies the response of the oscillator to the force  $I(\nu t)$ . This function is  $2\pi$ -periodic in the phase variables  $\varphi$  and  $\psi = \nu t$ , and generally also depends on the parameters and the shape of the forcing. In the first approximation in  $\varepsilon$ , this function, according to the perturbation theory,<sup>18</sup> is proportional to  $\varepsilon$  and does not depend on the driving frequency  $\nu$ :

$$Q(\varphi, \nu t; \varepsilon, \nu) \approx \varepsilon Q_0(\varphi, \nu t). \quad (3)$$

In the higher-order approximations, the coupling shall be represented by a power series in  $\varepsilon$ . Derivation of the high-order terms remains a theoretical challenge and we can expect that these terms can also depend on the driving frequency  $\nu$ . Notice that generally the coupling function can possess a constant term that cannot be separated from the natural frequency; we can take this into account by writing  $\omega = \omega(\varepsilon)$  in Eq. (2). We expect this equation to be valid as long as the phase space of the forced system possesses an attractive smooth 2-dimensional torus spanned by  $\varphi$  and  $\psi = \nu t$ , see Ref. 19 for a mathematical treatment and Ref. 3 for a discussion.

Notice that quite often the phase dynamics equation can be written in the Winfree form<sup>20,21</sup> with  $Q(\varphi, \psi) = Z(\varphi)I(\psi)$ . This representation of the coupling function as the product of the phase response curve  $Z$  and the external force  $I$  has certain advantages, e.g., the knowledge of  $Z$  allows studying a response to different forcing waveforms. However, this representation is not general and therefore in the rest of the paper, we use the phase dynamics model in the form of Eq. (2). As explained below, the knowledge of the phase dynamics model (2) provides the Arnold tongues for the original system.

### A. Determination of the synchronization domain from the phase dynamics

An analytical derivation of Eq. (2) for sufficiently large forcing represents an unsolved problem and anyway requires knowledge of the original dynamical model. However, a *numerical reconstruction* of this equation from observations of an unknown system with known input is a relatively simple task. Since the parameters of the force are assumed to be controlled in the experiment, the phase  $\psi$  of the force can be considered as given. In its turn, the phase  $\varphi$  can be estimated from an observed output of the oscillator, e.g., by means of the Hilbert Transform. Then, Eq. (2) can be reconstructed from known  $\varphi$  and  $\psi$ , as explained below in Subsection II B.

For presentation of our approach, we assume for the moment that the coupling function  $Q$  is already known and that it has been reconstructed for the forcing with parameters  $\nu_*$ ,  $\varepsilon_*$ . Thus, the noise-free dynamics obeys

$$\dot{\varphi} = \omega(\varepsilon_*) + Q(\varphi, \nu_* t; \varepsilon_*, \nu_*). \quad (4)$$

The key assumption behind this approach is that the form of the coupling function weakly depends on  $\nu_*$  and therefore we can use this function in order to describe the oscillator dynamics for different driving frequencies  $\nu$ . Hence, considering the driving frequency  $\nu$  in Eq. (4) as a free parameter, we write, with account of  $\dot{\psi} = \nu$ :

$$\frac{d\varphi}{d\psi} = \frac{\omega(\varepsilon_*) + Q(\varphi, \psi; \varepsilon_*, \nu_*)}{\nu}. \quad (5)$$

We solve this equation numerically for values  $\nu$  within some range. In this way, we find the phase increment  $\Delta\varphi$ , corresponding to the increment  $\Delta\psi = 2\pi N$ ,  $N \gg 1$ , and obtain the frequency of the driven oscillator  $\Omega(\nu, \varepsilon_*) = \Delta\varphi/\Delta t = \nu\Delta\varphi/\Delta\psi$ . Analyzing the function  $\Omega(\nu, \varepsilon_*)$ , we obtain the synchronous domain as an interval of  $\nu$ , where the locking condition  $n\Omega = m\nu$  holds for some integers  $n, m$ . Then, the experiment can be repeated for different values of the amplitude  $\varepsilon_*$  to yield the Arnold tongue.

Summarizing, one needs just one measurement for each amplitude of the forcing to reconstruct the whole synchronization domain. Below, we will also discuss a possibility to reconstruct the whole Arnold tongue from a single measurement, i.e., just for one pair  $(\varepsilon^*, \nu^*)$ .

### B. Reconstruction of coupling functions from data

Here, we briefly outline the steps of the reconstruction of the coupling function from data. The detailed description of the technique can be found in the [Appendix](#).

1. The first stage is estimation of the oscillator's instantaneous phase from the time series. We accomplish this task in two steps. First, we obtain an initial estimate of the phase (a protophase) by means of the Hilbert Transform of an observable of the forced oscillator, recorded as a time series  $x(t)$ . Next, we perform a protophase-to-phase transformation<sup>22,23</sup> which yields an invariant, i.e., independent of the chosen observable, phase  $\varphi(t)$ .
2. At the next stage, we compute numerically  $\dot{\varphi}(t)$  using a local polynomial approximation with the help of a Savitzky-Golay filter.
3. Finally, we fit  $\dot{\varphi}$  by a function  $\omega + Q(\varphi, \psi)$ , where  $\psi = \nu t$ . Naturally, the function  $Q$  is  $2\pi$ -periodic with respect to both arguments. This fit can be accomplished in several ways; here we use a kernel estimation technique.<sup>24,25</sup>

### C. Determination of Arnold tongues by the standard technique

In order to test our results, we first compute the true synchronization domain (the Arnold tongue) of each model using the standard technique. For this purpose, we simulate a driven oscillator for various values of the amplitude and the frequency of the external force. Namely, we scan the frequency  $\nu$  for a number of fixed values of the amplitude  $\varepsilon$ , and

compute the corresponding frequency of the driven system,  $\Omega = \Omega(\varepsilon, \nu)$ . For these fixed values of  $\varepsilon$ , the synchronization domain corresponds to the plateau in the plot of  $\Omega - \nu$  vs.  $\nu$ , i.e., to the frequency interval, where  $\Omega = \nu$ . Practically, for periodic oscillators we determine this interval using the condition  $|\Omega - \nu| < 10^{-5}$ . In the case of a high-order locking  $n\Omega = m\nu$ , the condition  $|n\Omega - m\nu| < 10^{-5}$  shall be used. For noisy and chaotic oscillators, we present the full dependence of  $\Omega - \nu$  on  $\nu$ , because there the Arnold tongue is not defined as strict as in the periodic case.

### III. RESULTS

Here, we present the results of numerical experiments with periodic, noisy, and chaotic oscillators.

#### A. Periodic oscillator

Our basic model is the Rayleigh oscillator, subject to an external harmonic force:

$$\ddot{x} - \mu(1 - \dot{x}^2)\dot{x} + x = \varepsilon \cos(\nu t). \quad (6)$$

In the following, the nonlinearity parameter is fixed as  $\mu = 4$ ; for this value, the limit cycle is quite stable and we expect the phase approximation to be valid for reasonably large values of  $\varepsilon$ . Let us first concentrate on the case of 1 : 1 locking, when  $\nu \approx \omega$ .

First, we determine the true synchronization domain for a number of fixed values of the amplitude  $\varepsilon$  of the external force (these values are:  $\varepsilon = 0.01, 0.02, \dots, 0.05, 0.1, 0.2, \dots, 0.8$ ). The resulting Arnold tongue is shown by bold gray curves in Fig. 1. As expected from the theory, for small amplitudes, where the coupling function can be further reduced to a function of the phase difference, the borders of the domain are straight lines.

Next, we reconstruct the synchronization domain for each value of  $\varepsilon$ . To this end, we record the output of the system for a fixed value of the driving frequency  $\nu_*$ . From this single measurement we reconstruct the coupling function  $Q$ , as described in Sec. II B, using the  $x$ -variable, sampled with the time step 0.1, as an observable. Then, we use  $Q$  to solve numerically Eq. (5), considering there  $\nu$  as a free parameter.<sup>26</sup> In this way, we obtain the dependence  $\Omega(\nu)$ , and reconstruct the synchronization interval for the chosen value of  $\varepsilon_*$ . Repeating this procedure for different  $\varepsilon_*$ , we reconstruct the Arnold tongue.

The results are shown in Fig. 1 for two tests. In the first one, we choose the driving frequency close to the left border of the tongue, while in the second test we take it close to the right border. We see that the reconstruction is nearly perfect for the border closest to the driving frequency used for the reconstruction, even for large forcing amplitudes where the first-order phase approximation (3) is definitely not valid. The other, distant side of the tongue, is recovered quite well for the amplitudes as large as  $\varepsilon \lesssim 0.3$ .

According to the phase reduction theory, for a weak forcing, the coupling function is simply rescaled with the amplitude of the force, see Eq. (3). Hence, driving the system with only one value of the frequency and of the amplitude shall be sufficient in order to determine the whole synchronization domain in the first-order phase approximation. This means

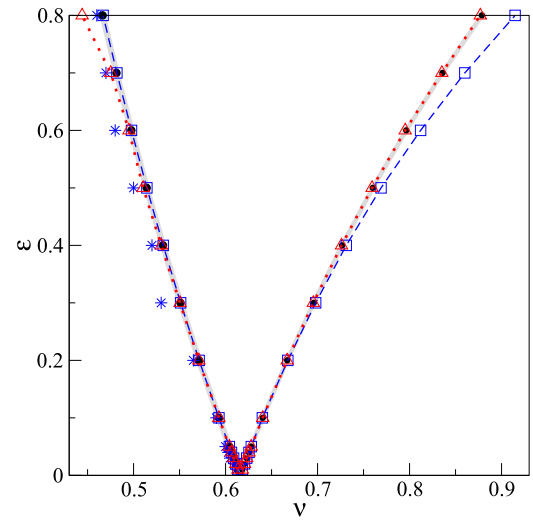


FIG. 1. Synchronization domain of the harmonically driven Rayleigh oscillator (6). The true domain is shown by bold gray lines; it has been determined for the discrete values of the forcing amplitudes  $\varepsilon$ , indicated by filled circles. Blue squares (connected by the blue dashed line) show the borders of the tongue reconstructed for each  $\varepsilon$  from a single measurement, where the frequency of the forcing was taken to be to the left of the domain (blue stars). We see that this technique perfectly recovers the left border of the domain. For the right border, the agreement is very good for the amplitudes  $\varepsilon \lesssim 0.3$ , while an essential deviation is observed for stronger forcing, where the assumption of independence of the coupling function on the driving frequency is slightly violated. Red triangles (connected by the red dotted line) show similar results obtained for the driving frequencies taken to the right of the tongue. Correspondingly, here the right border is reproduced very well.

that after determining the coupling function  $Q(\varphi, \psi; \varepsilon_*, \nu_*)$  for a particular forcing, we use an equation

$$\frac{d\phi}{d\psi} = \frac{\omega(\varepsilon_*)}{\nu} + \frac{\varepsilon Q(\varphi, \psi; \varepsilon_*, \nu_*)}{\nu \varepsilon_*}. \quad (7)$$

to find the synchronization domain at other values  $(\varepsilon, \nu)$ .

We illustrate this idea in Fig. 2. Here, along with the true tongue, we show the reconstructions for two different pairs of the forcing parameters  $\varepsilon_*$  and  $\nu_*$ . As expected, the coincidence is very good for small  $\varepsilon_*$ , where the first-order phase approximation is valid and the theory predicts a triangular shape of the tongue, while the deviation of the estimated borders from the true ones is essential for large  $\varepsilon_*$ .

In the first tests, we have chosen the driving frequency to be quite close to the border of the synchronization domain. Now, we check how important it is. In Fig. 3, we show the estimates of the left,  $\nu_l$ , and right,  $\nu_r$ , borders in dependence on the driving frequency  $\nu_*$ , for two different values of the amplitude. According to the theory, if the phase reduction in the first approximation is valid, there shall be no frequency dependence, and, indeed, it is marginal for  $\varepsilon = 0.01$ , while it becomes essential for stronger driving (see also Ref. 27).

Finally, we mention that the technique works in the same way for high-order synchronization ratios. We have checked this by subjecting the Rayleigh oscillator to a harmonic force with the amplitude  $\varepsilon_* = 0.05$  and frequency  $\nu_* = 1.8$ . Using this single measurement, we perfectly reproduced the synchronization domain with 3 : 1 locking in the frequency interval  $1.816 \lesssim \nu \lesssim 1.88$ .

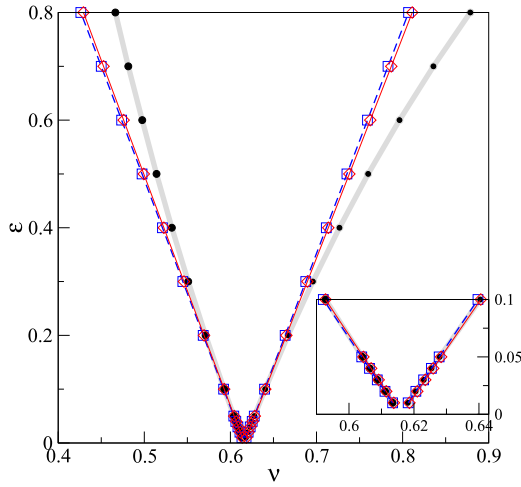


FIG. 2. Synchronization domain of the harmonically driven Rayleigh oscillator (6). The true domain is shown by bold gray lines; it has been determined for the discrete values of the forcing amplitudes  $\varepsilon$ , indicated by filled circles. The domains obtained according to Eq. (7) from a single measurement at  $\varepsilon_* = 0.01$ ,  $\nu_* = 0.612$ , and a measurement at  $\varepsilon_* = 0.1$ ,  $\nu_* = 0.59$  are shown by blue squares (connected by the dashed line) and by open red diamonds (solid line), respectively. The reconstructed coupling function for the latter case is shown in Fig. 7(a). The inset shows a zoom of the tongue for small values of  $\varepsilon$ .

### B. Noisy oscillator

Now, we consider a harmonically forced noisy Rayleigh oscillator:

$$\ddot{x} - \mu(1 - \dot{x}^2)\dot{x} + x = \varepsilon \cos(\nu t) + \xi(t), \quad (8)$$

where  $\xi(t)$  is Gaussian white noise with zero mean and intensity  $D$ . The plot  $\Omega - \nu$  vs  $\nu$  for the noise-free system, obtained in a standard way is shown by wide gray curve in Fig. 4. The plateau in this plot indicates the true domain of 1:1 locking. We also show here the corresponding  $\Omega - \nu$  vs.  $\nu$  plots for the noisy oscillator for two different noise intensities. These curves illustrate the well-known fact that the domain of synchrony for the noisy system is not well-defined and can be determined only approximately.<sup>3</sup> Next, we perform the same

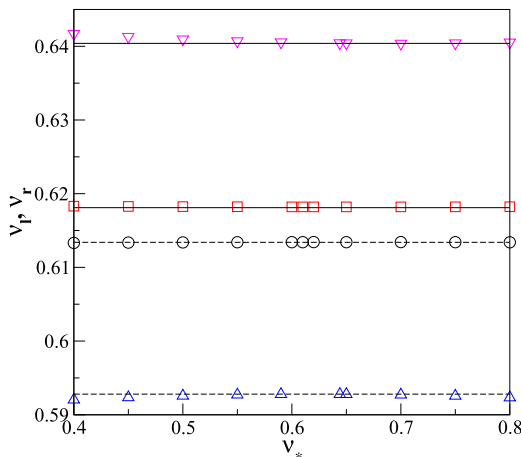


FIG. 3. Dependence of the estimate for the left,  $\nu_l$ , and the right,  $\nu_r$ , borders of the synchronization domain on the frequency  $\nu_*$  of the forcing. The results are shown for  $\varepsilon_* = 0.01$  (black circles for  $\nu_l$ , red squares for  $\nu_r$ ) and for  $\varepsilon_* = 0.1$  (blue triangles up for  $\nu_l$ , magenta triangles down for  $\nu_r$ ). The true values of  $\nu_l$  and  $\nu_r$  are shown by dashed and solid lines, respectively.

analysis as described in the Sec. III A: from the phases of the oscillator and of the force we recover the coupling function. Since in fact we fit the instantaneous frequency  $\dot{\varphi}$  by a function of  $\varphi, \psi$ , the random perturbations are washed out due to averaging. Therefore, we expect that the obtained coupling function is close to that of the noise-free system. This expectation is confirmed by Fig. 4.

For noise intensity  $D = 0.02$ , the recovered synchronization domain is hardly distinguishable from the true one. For  $D = 0.05$ , the results are not perfect, though our technique provides a better result from a single measurement than the standard technique from many measurements. Notice that the latter example is a quite tough test, since the noise here is quite strong if compared to the amplitude of the regular driving force.

### C. Chaotic system

For the next example, we take the chaotic Rössler oscillator.<sup>28</sup> The equations of the driven system read

$$\begin{aligned} \dot{x} &= y - z + \varepsilon \cos(\nu t), \\ \dot{y} &= x + 0.15y, \\ \dot{z} &= 0.4 + z(x - 8.5). \end{aligned} \quad (9)$$

It is known that many chaotic systems, and the Rössler system in particular, admit an approximate description in terms of phases and the appropriately introduced average frequency can be locked to an external force or to another oscillator.<sup>29,30</sup> This effect, known as phase synchronization of chaos, has certain similarity with synchronization of noisy oscillators. Therefore, we perform the same test, as with the noisy Rayleigh oscillator. The phase of the Rössler oscillator was obtained from the observable  $x(t)$  by means of the Hilbert Transform.

The results are presented in Fig. 5. Here, again we show the true synchronization domain and its reconstructions from single measurements for  $\nu_* = 1.01$  and for  $\nu_* = 1.06$ ; the forcing amplitude was  $\varepsilon_* = 0.2$ . Like for the periodic oscillators above, the prediction is definitely better for the synchronization domain border closest to the frequency of the driving used for the reconstruction.

### D. Oscillator in a network

With the following example, we illustrate some limitations of our approach. We again consider the Rayleigh oscillator, but now it is affected by two harmonic forces and a random perturbation:

$$\ddot{x} - \mu(1 - \dot{x}^2)\dot{x} + x = \varepsilon \cos(\nu t) + \varepsilon_1 \cos(\nu_1 t) + \xi(t). \quad (10)$$

The first term on the r.h.s. represents the known force which parameters  $\varepsilon, \nu$  we can control and which phase we can obtain, while the second and third terms simulate the unknown regular and stochastic inputs, respectively. The latter is again Gaussian noise with zero mean and intensity  $D$ . The task is to determine the domain of entrainment by the controlled force  $\varepsilon \cos(\nu t)$ , i.e., as if the second regular force and the stochastic perturbation were switched off.



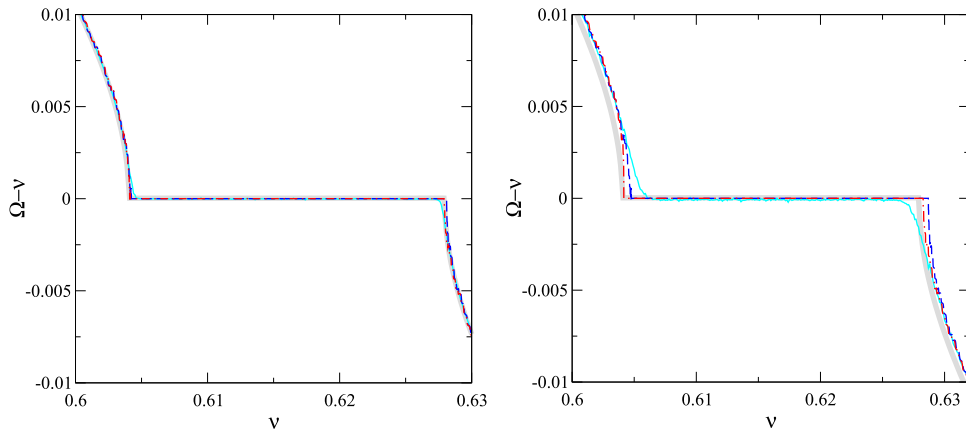


FIG. 4. The observed frequency  $\Omega$  vs the driving one for the noisy Rayleigh oscillator (6) for noise intensity  $D = 0.02$  (left panel) and  $D = 0.05$  (right panel). The bold gray curve was obtained by the standard technique, i.e., by scanning the frequency of the force,  $\nu$ , for the noise-free system; this curve provides the true synchronization domain. The cyan solid curve illustrates synchronization of the noisy oscillator. The blue dashed and red dashed-dotted curves present the synchronization domain reconstructed from a single measurement by means of Eq. (5), for  $\nu_* = 0.6$  and  $\nu_* = 0.63$ , respectively. The forcing amplitude was  $\varepsilon_* = 0.05$ .

Let us consider the phase dynamics model for Eq. (8). In the first-order approximation in  $\varepsilon$  it takes the form

$$\dot{\varphi} = \omega + \varepsilon Q(\varphi, \nu t) + \varepsilon_1 Q_1(\varphi, \nu_1 t) + Q_n(\varphi, \xi). \quad (11)$$

In the higher-order approximation, there shall appear the cross terms, e.g., depending on the three phases  $\varphi$ ,  $\nu t$ , and  $\nu_1 t$ . If the coupling function  $Q$  and the frequency  $\omega$  were known exactly, then, it would be possible to solve numerically the equation

$$\dot{\varphi} = \omega + \varepsilon Q(\varphi, \nu t)$$

for different  $\nu$  and to find in this way the desired locking region, at least for weak forcing when the first approximation (11) is valid. Omitting the two last terms in Eq. (11) is equivalent to “switching off” the corresponding perturbations. However, we do not know  $\omega$  and  $Q$ , but can only estimate them from data in the presence of unknown perturbations. Fitting the right hand side of Eq. (11) by a function of  $\varphi$ ,  $\psi = \nu t$ , we perform an effective averaging of the unobserved terms. However, this averaging can yield a constant term of the order of  $\varepsilon_1$  and  $D$ .

We illustrate these considerations with the results of numerical experiments, shown in Fig. 6. Here, we compare

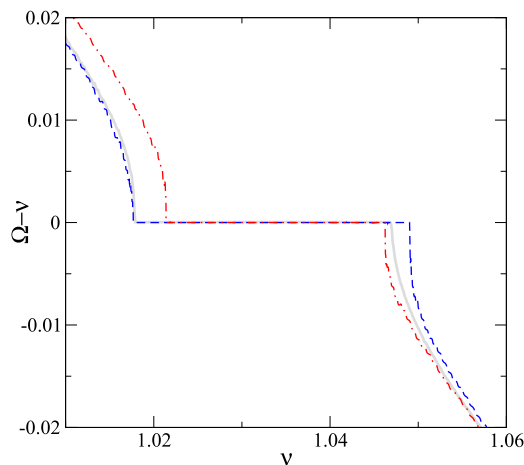


FIG. 5. The observed frequency  $\Omega$  of the chaotic Rössler oscillator (9), for  $\varepsilon = 0.2$ . The bold gray curve was obtained by the standard technique, i.e., by scanning the frequency of the force,  $\nu$ ; this curve provides the true synchronization domain. The blue dashed and red dashed-dotted curves present the synchronization domain reconstructed by means of phase dynamics modeling for  $\nu_* = 1.01$  and  $\nu_* = 1.06$ , respectively. The corresponding coupling function for the latter case is shown in Fig. 7(b).

the true synchronization region obtained for  $\varepsilon_1 = 0$ ,  $D = 0$ , with the corresponding curve computed for the case when the uncontrolled force with  $\varepsilon_1 = 0.05$  and  $\nu_1 = 0.5$  is present. One can see that the reconstruction indeed provides the tongue with a small error: the effect of the unobserved force cannot be completely eliminated. Thus, for a weak unobserved force, we obtain the tongue with a small bias, as can be seen in Fig. 6. It is important that this bias depends not only on  $\varepsilon_1$  but also on  $\nu_1$ : if the frequency of the unobserved force is far away from the tongue, then its effect is marginal. For example, for  $\nu_1 = 0.2$ , the reconstruction is very good. Notice that if the second force can be measured as well, and its phase can be determined, then one can reconstruct both regular terms in the phase model (cf. Ref. 31) and thus improve the results.

#### IV. DISCUSSION

In summary, we have suggested an approach for an efficient determination of the synchronization domains of an oscillator in an active experiment where the system is forced and the parameters of the force can be controlled. The technique is applicable to any self-sustained periodic oscillator, quasilinear or relaxational, as long as the measured observable allows for estimation of an instantaneous phase. A

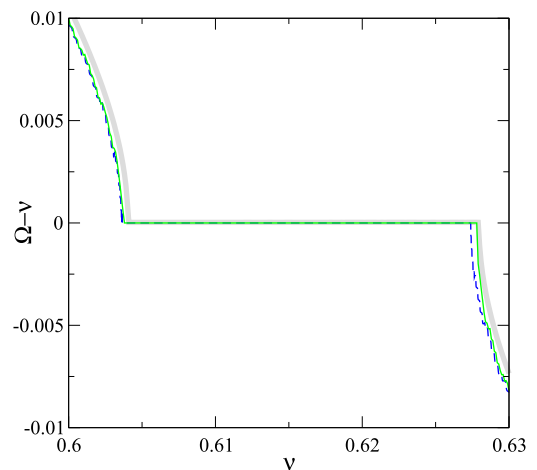


FIG. 6. Rayleigh oscillator driven by two forces Eq. (8). The blue dashed and the green solid curves present the reconstructed values of the observed frequency  $\Omega$  for  $\nu_* = 0.6$  and for  $D = 0$  and  $D = 0.02$ , respectively. The bold gray curve was obtained by a standard technique.

counter-example is, e.g., neuronal spiking, where the action potential is not resolved and the signal between the spikes is nearly constant and dominated by noise, so that in fact only a point process is available. However, if the experimental trace from a spiking neuron (or from a spontaneously beating an atrial pacemaker cell) is a continuously varying, though a rapidly changing signal (cf., e.g. solution of the Morris-Lecar neuronal model), then the phase estimation can be performed as described in the paper, and the Arnold tongue can be computed. Next, we mention that networks of interacting oscillators, in particular of spiking neurons, can exhibit collective oscillations. Such a collective mode behaves like a macroscopic oscillator that can be entrained by an external force,<sup>32,33</sup> and the presented approach applies here as well. Finally, we notice that the forcing does not have to be a harmonic one; the technique works similarly for a periodic force of an arbitrary form.

The main advantage of the approach is that, in contrast to the standard technique, it requires only a few observations. This makes the method especially useful in investigation of life systems, where it may be highly desirable to reduce the intervention, or the time interval, where the system can be considered as stationary is short. For an illustration of the performance, let us discuss Fig. 5. Here, 600 frequency points have been used to construct the tongue by the standard technique. With our approach, we can use a few frequency points to obtain first a rough estimate of the locking domain, and then we need further several points, taken near each border of the tongue, to improve the reconstruction. Thus, about 50 times less measurement points are required for a reliable determination of the tongue.

For a practical application of this technique, we suggest the following strategy. First, one shall perform a measurement for a weak forcing and, assuming that the first-order phase approximation is valid, reconstruct the whole Arnold tongue from this single measurement (cf. Fig. 2). Most likely this tongue is only a rough approximation of the true one, especially for large  $\varepsilon$ , but this first estimation can be now improved by measurements with a larger forcing amplitude and with the frequency  $\nu$  of the force chosen close to the border of the tongue (but outside of it). For a strong forcing, this closeness of the frequency is important because the coupling function becomes dependent on  $\nu$ , and that is where the first rough approximation is helpful. However,  $\nu$  shall be not too close to the border. Indeed, if the system is very close to synchrony, then the finite-length trajectory does not cover the torus formed by phases  $\varphi$  and  $\psi$ , and the reconstruction of the function of these two variables is hampered. We suggest always to check this by plotting  $\psi$  vs.  $\varphi$  (both phases shall be wrapped to  $0, 2\pi$  interval) and verifying that the points cover the  $2\pi \times 2\pi$  square.

We emphasize that our approach can be also useful in the case of passive experiments, when only observations of the system under free-running conditions are possible. Indeed, suppose we observe the outputs of two interacting, though not synchronized, oscillators. Considering, say, the second unit as a driver, we can reconstruct the phase dynamics of the first unit from this single observation, and roughly predict synchronization properties of the driven system.

An essential feature of our approach is that it efficiently works with noise-perturbed oscillators and allows one to reveal the synchronization properties of the corresponding noise-free system. We underline that the mechanism behind this is not a usual filtering. Indeed, if the phase dynamics equation (2) is obtained, then its deterministic part can be solved in order to generate the output of the oscillator if there were no noise at all. This “switching off” of a certain input is a particular case of a procedure for separating different forcing terms in the dynamics, called dynamical disentanglement. It has been recently applied to the analysis of interaction between cardiovascular and respiratory systems<sup>24,34</sup> and provided a separation of the respiratory-related and the non-respiratory related heart rate variability with the help of the phase dynamics reconstruction.

## ACKNOWLEDGMENTS

The work was supported by ITN COSMOS (funded by the European Union Horizon 2020 Research and Innovation Programme under the Marie Skłodowska-Curie Grant Agreement No. 642563). Numerical part of this work was supported by the Russian Science Foundation (noisy oscillations, Grant No. 14-12-00811 and chaotic oscillations, Grant No. 17-12-01534).

## APPENDIX: DETAILS OF PHASE MODEL INFERENCE FROM DATA

All building blocks of the algorithm are implemented as functions in “Data Analysis with Models of Coupled Oscillators” Matlab toolbox (DAMOCO) and can be found here.<sup>35</sup>

The initial step in our technique is the estimation of the phases from data. Suppose, we have a measurement of an observable of the forced oscillator,  $x(t)$ . First, we compute the Hilbert transform  $x_H(t)$  of  $x(t)$  and take the argument  $\theta(t)$  of the complex signal  $[x(t) - x^*] + i[x_H(t) - x_H^*]$  as the protophase. Here, the coordinates  $x^*, x_H^*$  of the origin in the complex plane shall be chosen in such a way that all loops of the trajectory revolve around this point. Typically, the average values can be chosen for  $x^*, x_H^*$ , but generally a visual inspection of the trajectory in the complex plane is recommended. Further discussion and examples can be found in Ref. 3. Practically,  $x(t)$  and  $\theta(t)$  are given as time series sampled with a constant time interval, i.e., as  $x(t_k)$  and  $\theta(t_k)$ . This step can be performed with the help of the DAMOCO function `co_hilbproto`.

We notice that the phase estimation via the Hilbert transform fails if the waveform is complex (several maxima over the period), so that the representation in the Hilbert plane yields a trajectory with self-intersections. A representative example of such a signal is an electrocardiogram. As far as we know, there is no universal recipe for treating such time series and *ad hoc* techniques are used, see, e.g., Refs. 23 and 24.

Next, we transform the protophase  $\theta$  to the phase  $\varphi$  using the technique developed in Refs. 22 and 23. The idea behind this transformation reflects the property of the true phase of an autonomous system to grow uniformly in time,  $\dot{\varphi} = \omega$ , while

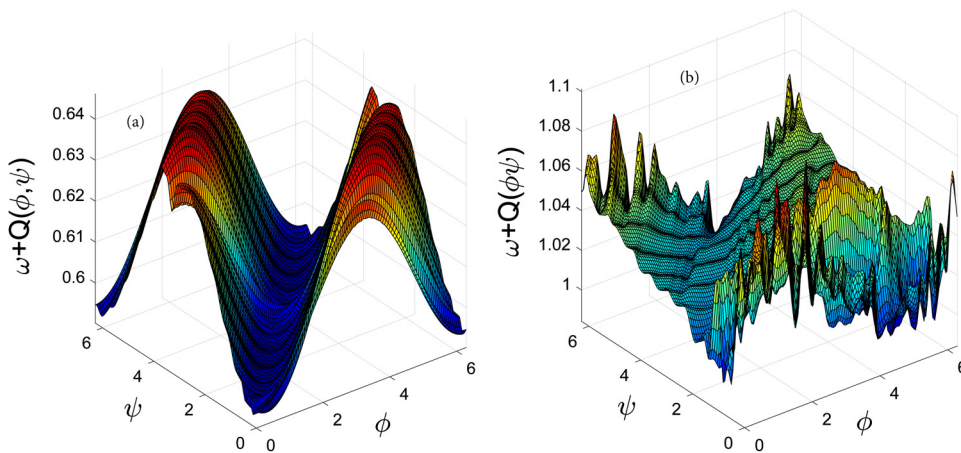


FIG. 7. The reconstructed coupling functions for the noise-free Rayleigh oscillator (a) and the chaotic Rössler oscillator (b).

the evolution of an angular variable (protophase) is monotonic but not generally uniform, i.e.,  $\dot{\theta} = f(\theta)$ . The one-to-one invertible transformation<sup>22,23</sup> removes all the variations in the phase growth that depend on the phase of the oscillator, and preserves all the variations that are due to the external force and therefore depend on its phase  $\psi$ . The transformation reads

$$\varphi = \theta + 2 \sum_{n=1}^{\infty} \text{Im} \left[ \frac{S_n}{n} (e^{in\theta} - 1) \right], \quad (\text{A1})$$

where  $S_n$  are Fourier coefficients of the probability density function of  $\theta$ . They can be directly computed from the time series of  $\theta_k$ ,  $k = 1, \dots, N$  as  $S_n = N^{-1} \sum_k e^{in\theta_k}$ . The number  $n$  of Fourier coefficients can be either chosen sufficiently large, e.g., between 50 and 100, or can be taken according to an optimization scheme, see Ref. 24; here we used the latter option. The corresponding toolbox function is `co_fbtrT`.

Numerical differentiation of the phase is performed by means of a Savitzky-Golay polynomial filter.<sup>36</sup> We used the DAMOCO function `co_phidot2` with fourth order polynomial and the window length 0.12. (The results are rather insensitive to the choice of these parameters.)

Finally, we obtain the coupling function  $Q$  by fitting  $\dot{\varphi}$  by a function of  $\varphi$  and  $\psi$ , using the kernel density estimation<sup>24</sup> (toolbox function `co_kcplfct1`). For this purpose, we choose a rectangular  $m \times m$  grid on the square  $0 \leq \varphi < 2\pi$ ,  $0 \leq \psi < 2\pi$ . Let  $\varphi_g, \psi_g$  be one of the points on this grid. Then, the function at this point is estimated as

$$Q(\varphi_g, \psi_g) = \frac{\sum_{k=1}^N \dot{\varphi}(t_k) K[\varphi_g - \varphi(t_k), \psi_g - \psi(t_k)]}{\sum_{k=1}^N K[\varphi_g - \varphi(t_k), \psi_g - \psi(t_k)]},$$

where the smoothing kernel is

$$K(x, y) = \exp \left[ \frac{m}{2\pi} (\cos x + \cos y) \right].$$

In all computations, we used  $m = 100$ . Examples of the reconstructed functions are given in Fig. 7.

<sup>1</sup>B. van der Pol and J. van der Mark, “The heartbeat considered as a relaxation oscillation and an electrical model of the heart,” *Phil. Mag.* **6**, 763–775 (1928).

<sup>2</sup>E. V. Appleton, “The automatic synchronization of triode oscillator,” *Proc. Cambridge Phil. Soc. (Math. Phys. Sci)* **21**, 231–248 (1922).

<sup>3</sup>A. Pikovsky, M. Rosenblum, and J. Kurths, *Synchronization. A Universal Concept in Nonlinear Sciences* (Cambridge University Press, Cambridge, 2001).

<sup>4</sup>S.-B. Shim, M. Imboden, and P. Mohanty, “Synchronized oscillation in coupled nanomechanical oscillators,” *Science* **316**, 95 (2007).

<sup>5</sup>M. Abel and S. Bergweiler, “Synchronization of organ pipes: Experimental observations and modeling,” *J. Acoust. Soc. Am.* **119**, 2467–2475 (2006).

<sup>6</sup>M. Abel and S. Bergweiler, “Synchronization of higher harmonics in coupled organ pipes,” *Int. J. Bifurcat. Chaos* **17**, 3483–3491 (2007).

<sup>7</sup>D. P. Rosin, D. Rontani, and D. J. Gauthier, “Synchronization of coupled boolean phase oscillators,” *Phys. Rev. E* **89**, 042907 (2014).

<sup>8</sup>H. Willaime, V. Barbier, L. Kloul, S. Maine, and P. Tabeling, “Arnold tongues in a microfluidic drop emitter,” *Phys. Rev. Lett.* **96**, 054501 (2006).

<sup>9</sup>O. Mondragón-Palomino, T. Danino, J. Selimkhanov, L. Tsimring, and J. Hasty, “Entrainment of a population of synthetic genetic oscillators,” *Science* **333**, 1315–1319 (2011). <http://science.sciencemag.org/content/333/6047/1315.full.pdf>.

<sup>10</sup>S. Rzezcinski, N. B. Janson, A. G. Balanov, and P. V. E. McClintock, “Regions of cardiorespiratory synchronization in humans under paced respiration,” *Phys. Rev. E* **66**, 051909 (2002).

<sup>11</sup>M. D. Prokhorov, V. I. Ponomarenko, V. I. Gridnev, M. B. Bodrov, and A. B. Bespyatov, “Synchronization between main rhythmic processes in the human cardiovascular system,” *Phys. Rev. E* **68**, 041913 (2003).

<sup>12</sup>M. Levy, A. Molzon, J.-H. Lee, J.-w. Kim, J. Cheon, and D. Bozovic, “High-order synchronization of hair cell bundles,” *Sci. Rep.* **6**, 39116 (2016).

<sup>13</sup>A. Notbohm, J. Kurths, and C. Herrmann, “Modification of brain oscillations via rhythmic light stimulation provides evidence for entrainment but not for superposition of event-related responses,” *Front. Hum. Neurosci.* **10**, 10 (2016).

<sup>14</sup>E. Lowet, M. J. Roberts, A. Peter, B. Gips, and P. D. Weerd, “A quantitative theory of gamma synchronization in macaque v1,” *eLife* **6**, e26642 (2017).

<sup>15</sup>G. Penelet and T. Biwa, “Synchronization of a thermoacoustic oscillator by an external sound source,” *Am. J. Phys.* **81**, 290 (2013).

<sup>16</sup>J. L. Perez Velazquez, R. Guevara Erra, and M. Rosenblum, “The epileptic thalamocortical network is a macroscopic self-sustained oscillator: Evidence from frequency-locking experiments in rat brains,” *Sci. Rep.* **5**, 8423 (2015).

<sup>17</sup>A. Erzberger, G. Hampp, A. E. Granada, U. Albrecht, and H. Herzog, “Genetic redundancy strengthens the circadian clock leading to a narrow entrainment range,” *J. R. Soc. Interface* **10**, 20130221 (2013). <http://rsif.royalsocietypublishing.org/content/10/84/20130221.full.pdf>.

<sup>18</sup>Y. Kuramoto, *Chemical Oscillations, Waves and Turbulence* (Springer, Berlin, 1984).

<sup>19</sup>V. S. Afraimovich and L. P. Shilnikov, “Invariant two-dimensional tori, their destroying and stochasticity,” in *Methods of Qualitative Theory of Differential Equations* (Gorki, 1983), pp. 3–28 (in Russian) [Amer. Math. Soc. Transl. Ser. 2 **149**, 201–212 (1991)].

<sup>20</sup>A. T. Winfree, “Biological rhythms and the behavior of populations of coupled oscillators,” *J. Theor. Biol.* **16**, 15 (1967).

<sup>21</sup>A. T. Winfree, *The Geometry of Biological Time* (Springer, Berlin, 1980).

<sup>22</sup>B. Kralemann, L. Cimponeriu, M. Rosenblum, A. Pikovsky, and R. Mrowka, “Uncovering interaction of coupled oscillators from data,” *Phys. Rev. E* **76**, 055201 (2007).

- <sup>23</sup>B. Kralemann, L. Cimponeriu, M. Rosenblum, A. Pikovsky, and R. Mrowka, "Phase dynamics of coupled oscillators reconstructed from data," *Phys. Rev. E* **77**, 066205 (2008).
- <sup>24</sup>B. Kralemann, M. Frühwirth, A. Pikovsky, M. Rosenblum, T. Kenner, J. Schaefer, and M. Moser, "In vivo cardiac phase response curve elucidates human respiratory heart rate variability," *Nat. Commun.* **4**, 2418 (2013).
- <sup>25</sup>Y.-C. Chen, "A tutorial on kernel density estimation and recent advances," *Biostat. Epidemiol.* **1**, 161–187 (2017).
- <sup>26</sup>We use the Euler scheme with the step equal to the step of the grid where the function  $Q$  is known, combined with an interpolation.
- <sup>27</sup>K. Blaha, A. Pikovsky, M. Rosenblum, M. Clark, C. Rusin, and J. Hudson, "Reconstruction of two-dimensional phase dynamics from experiments on coupled oscillators," *Phys. Rev. E* **84**, 046201 (2011).
- <sup>28</sup>O. E. Rössler, "An equation for continuous chaos," *Phys. Lett. A* **57**, 397–398 (1976).
- <sup>29</sup>M. G. Rosenblum, A. S. Pikovsky, and J. Kurths, "Phase synchronization of chaotic oscillators," *Phys. Rev. Lett.* **76**, 1804–1807 (1996).
- <sup>30</sup>A. S. Pikovsky, M. G. Rosenblum, G. V. Osipov, and J. Kurths, "Phase synchronization of chaotic oscillators by external driving," *Physica D* **104**, 219–238 (1997).
- <sup>31</sup>B. Kralemann, A. Pikovsky, and M. Rosenblum, "Reconstructing phase dynamics of oscillator networks," *Chaos* **21**, 025104 (2011).
- <sup>32</sup>L. M. Childs and S. H. Strogatz, "Stability diagram for the forced Kuramoto model," *Chaos* **18**, 043128 (2008).
- <sup>33</sup>A. A. Temirbayev, Y. D. Nalibayev, Z. Z. Zhanabaev, V. I. Ponomarenko, and M. Rosenblum, "Autonomous and forced dynamics of oscillator ensembles with global nonlinear coupling: An experimental study," *Phys. Rev. E* **87**, 062917 (2013).
- <sup>34</sup>Ç. Topçu, M. Frühwirth, M. Moser, M. Rosenblum, and A. Pikovsky, "Disentangling respiratory sinus arrhythmia in heart rate variability records," *Physiol. Meas.* **39**, 054002 (2018).
- <sup>35</sup>See [www.stat.physik.uni-potsdam.de/~mros/damoco2.html](http://www.stat.physik.uni-potsdam.de/~mros/damoco2.html).
- <sup>36</sup>W. H. Press, B. P. Flannery, S. A. Teukolsky, and W. T. Vetterling, *Numerical Recipes: The Art of Scientific Computing* (Cambridge University Press, Cambridge, 1986).